DIAGONAL COMPRESSION TESTING OF FRP-RETROFITTED UNREINFORCED CLAY BRICK MASONRY WALLETTES

Hamid Mahmood[1], S.M.ASCE
Jason M. Ingham[2], M.ASCE

Abstract

To address concerns regarding the seismic vulnerability of New Zealand unreinforced masonry (URM) buildings, a research program was undertaken to investigate the effectiveness of fiber reinforced polymer (FRP) systems as a seismic retrofit intervention for in-plane loaded URM walls that are prone to fail in a shear mode during earthquakes. Seventeen URM wallettes were retrofitted with either externally-bonded (EB) glass FRP fabrics, EB pultruded carbon FRP (CFRP) plates or near-surface mounted pultruded CFRP rectangular bars. The wallettes were tested by the application of a diagonal compressive force, and data was recorded for applied force and corresponding wall drift. Results were compared with five nominally identical unretrofitted wallettes. It was determined that the FRP systems substantially increased the shear strength of the wallettes. Significant increases in the pseudo-ductility and the toughness were also obtained, which are all considered to be important goals of any seismic retrofit intervention.

CE Database subject headings: Composite materials; Compression tests; Fiber reinforced polymers; Masonry; Rehabilitation; Seismic effects.

[1] Ph.D. Student, Department of Civil & Environmental Engineering, Faculty of Engineering, The University of Auckland, Private Bag 92019, Auckland Mail Centre, Auckland 1142, New Zealand.
Email: hmah012@aucklanduni.ac.nz.

[2] Associate Professor, Department of Civil & Environmental Engineering, Faculty of Engineering, The University of Auckland, Private Bag 92019, Auckland Mail Centre, Auckland 1142, New Zealand.
Email: j.ingham@auckland.ac.nz.

Introduction

Masonry has been the structural material of choice for centuries. However, historically unreinforced masonry (URM) structures have suffered extensive damage in earthquakes, such as in the 2005 Pakistan Earthquake (72,763 causalities) (Rossetto and Peiris 2009). The most significant of the past New Zealand earthquakes was the 1931 Hawke's Bay Earthquake that resulted in the deaths of 256 people (Dowrick 1998). Most of the dwellings in the affected area were constructed of solid clay brick URM, which was the most common construction material in New Zealand for commercial buildings at that time. Use of clay brick URM decreased after that earthquake and was also restricted in 1964 under government regulations following the introduction of the building bylaws NZS 1900 (Holmes 1965). The current New Zealand building stock consists of a significant number of mostly pre-1964 URM structures, and their presence constitutes a serious seismic hazard to New Zealand's citizens (Russell and Ingham 2010).

URM buildings can fail due to deficient strength of the walls when loaded in-plane (hereinafter referred as 'in-plane walls'), due to weak out-of-plane loaded walls, or due to inadequate diaphragms or diaphragm-wall connections (Bruneau 1994). The overall seismic performance of URM buildings depends on the capacity of in-plane walls to transfer lateral forces to the foundation and, hence, intact in-plane walls provide the post-earthquake stability necessary to avoid collapse of the entire structure. In an earthquake, the failure or deformation of in-plane walls can occur by the formation of X-shaped cracks (diagonal shear failure), by sliding of a portion of the wall generally along a bed joint (sliding shear deformation), by rocking about the wall toe, or by crushing of the wall toe (compression failure) (Magenes and Calvi 1997). The research reported here focused only on the shear modes of failure (diagonal shear failure and sliding shear deformation) of in-plane URM walls, recognizing especially that the diagonal shear failure mode of in-plane URM walls is commonly observed in earthquakes (Bruneau 1994, Javed et al. 2006).

Amongst other methods, seismic retrofit of deficient URM walls can be performed using either externally-bonded (EB) fiber reinforced polymer (FRP) fabrics (fiber sheets) and pultruded

plates or near-surface mounted (NSM) FRP bars. FRP systems are thinner and lighter, stronger, easier and faster to install and are less disruptive to building occupants during their installation than are conventional retrofit interventions such as shotcreting or structural frames. Most previous experimental research on FRP-retrofitted walls has focused on out-of-plane response (for example, Hamilton and Dolan 2001, Kuzik et al. 2003) and has shown that FRP materials are effective in increasing strength and ductility.

In-plane wall experimental research can be divided into (i) horizontal wall tests, in which a horizontal force is applied parallel to the top of the wall and (ii) diagonal compression tests, in which a force is applied along the wall diagonal to obtain shear failure. A number of researchers have performed horizontal wall tests (Alcaino and Santa-Maria 2008, Elgawady et al. 2005, Haroun and Mosallam 2002, Schwegler 1994, Seki et al. 2008, Stratford et al. 2004, To-Nan et al. 2006), reporting an increase in shear strength of between 18–190%. Obtaining a diagonal shear mode of failure was found to be difficult due to the tendency of isolated walls to rock and, in some cases, diagonal shear failure was obtained by restraining the wall from rocking or by precompressing the wall with a large magnitude axial load that is improbable in common URM buildings. Alternatively, force was applied along the wall diagonal to obtain a diagonal crack in a so-called diagonal compression test, which has been standardized (ASTM 2002) for URM wallettes measuring 1200 mm × 1200 mm, although a number of variations have been reported in the literature.

A summary of major diagonal compression testing that has been reported in the literature is presented in Table 1. It is evident that the application of an FRP retrofit system can enhance the shear strength of URM wallettes; however examples of both zero strength gain and of reduced strength have also been reported by some researchers (Marshall et al. 2000, Santa-Maria et al. 2004, Valluzzi et al. 2002) especially for wallettes with FRP applied on one face only. Many FRP orientations have been evaluated for in-plane wall retrofit, but different wallette orientations (see ‘γ’ in Table 1) and sizes, test setups and URM materials have been employed, which makes it difficult to compare and quantify the efficiency of different FRP retrofit systems. Also, most of the previously published

literature has focused on single-wythe masonry, which is not representative of real load-bearing URM construction, that typically is at least two wythes thick. When compared to concrete block masonry, less data is available for clay brick masonry, which is the prevalent URM material in New Zealand. Most previously published literature utilized new bricks, which may not adequately simulate the condition of masonry materials in old buildings, as is the case in New Zealand. In practice, FRP fabrics are usually anchored to the substrate, at least at edges, to prevent premature delamination, but previous tests have either not employed anchors or anchor details were not published. Generally, data for the increase in pseudo-ductility, toughness, and stiffness is either not available or has not been computed.

The objective of this research was to investigate the efficiency of FRP systems for improving the shear strength, pseudo-ductility, toughness and stiffness (being important goals in any seismic retrofit program) of URM walls likely to fail in a shear mode by addressing the gaps identified in previously reported literature. Seventeen FRP-retrofitted URM wallettes were tested to failure in a variation of the standard diagonal compression test setup. The results of the tests were compared with five nominally identical unretrofitted wallettes (Russell 2010), that were constructed in three stages (see Table 2 for details) on the same day as the corresponding FRP-retrofitted wallettes using similar masonry materials and were tested at approximately the same age as the corresponding retrofitted wallettes.

Experimental Program

Test Wallettes

Diagonal compression tests were performed on seventeen FRP-retrofitted solid clay brick masonry wallettes that were constructed and tested in three stages due to storage limitations in the testing hall. Stage 1 and stage 2 wallettes measured 1170 mm long × 1170 mm high, and stage 3 wallettes measured 1170 mm long × 1075 mm high. All wallettes were 225 mm (two wythes) thick. The wallette dimensions are listed in Table 2. In the nomenclature, ‘WT’ refers to WalleTtes, ‘G’ refers to glass FRP (GFRP) and ‘C’ refers to carbon FRP (CFRP). The wallettes were constructed in

the common bond pattern (Fig. 1) by experienced bricklayers, and the bond pattern and wall thicknesses were selected because of their high prevalence in New Zealand.

The wallettes were retrofitted with FRP materials, including EB uniaxial and biaxial GFRP fabrics and pultruded CFRP plates and NSM rectangular bars. Consistent with FRP retrofit practice to preserve the architectural façade, retrofitting was applied on one wallette face only, except for wallettes WTC7 and WTC9, which were retrofitted on both faces. The retrofit details for each wallette are depicted in Fig. 2 (also see Table 2).

Glass fabrics were applied using a multi-stage process. First, the wallette surface was ground, and any imperfections were filled with putty to obtain a near smooth surface. The primer epoxy coat was then applied to the wallette, and an epoxy-saturated glass fabric was positioned (Fig. 3) and worked against the wallette surface with rollers to achieve a good bond. The fabric was anchored to the wallette with glass fiber anchors (Fyfe Co. LLC 2009), which were first soaked with epoxy and then inserted into predrilled holes in the wallette through the first layer of fabric. The anchors were splayed on the surface of the first fabric layer, and the second fabric layer was applied afterwards to achieve an almost plane surface. For full surface coverage of GFRP fabrics, twelve anchors were placed at regular intervals around the fabric perimeter, and for retrofits that involved strips cut from GFRP fabrics, one anchor was placed at each end of the strip. A similar process was used for bonding CFRP plates to the wallette, however no anchors were used. After preparing the wallette surfaces by grinding, plates were bonded using a two-component epoxy. In wallettes WTC3 and WTC4, the plates were overlapped at the junction of two plates. For NSM application of rectangular bars, grooves were cut into the wallettes. Grooves were cleaned using an air gun and solvent, and were left to dry before being filled with epoxy. Epoxy was also applied to rectangular NSM bars, which were then inserted into the epoxy-filled grooves.

Materials

Masonry materials were selected to approximately replicate the conditions in old New Zealand URM buildings. Vintage clay bricks were extracted from pre-1964 New Zealand URM

buildings and cleaned before their use. These bricks were bonded together by means of weak (ASTM type O) mortar, which consisted of 1 part cement, 2 parts hydrated lime and 9 parts sand, by volume. This mortar mix was selected in an attempt to imitate possibly decayed mortar in historical buildings.

Compressive strength tests were conducted on mortar, bricks, and masonry during each wallette testing stage, and results (average values and standard deviations) are given in Table 3 for both the unretrofitted and retrofitted wallettes. Mortar compressive strength was determined by performing tests on 25 mm mortar cubes in accordance with ASTM C109-02 (ASTM 2002). The expected compressive strength for the used mortar mix was 1.5–2.4 MPa (ASTM 2003, Hendry et al. 1997), which compared well for stage 2 and stage 3. The wide variation in brick strength indicates high variability in the brick properties. Masonry compressive strength was determined from tests on masonry prisms conducted in accordance with ASTM C1314-03 (ASTM 2003). The compressive strength of masonry prisms was higher than the compressive strength of mortar cubes and lower than the compressive strength of bricks, which is consistent with previously reported results (Drysdale et al. 1999).

The manufacturer-provided properties of the GFRP fabrics (Fyfe Co. LLC 2009, 2010) and CFRP plates (Sika Corporation 2005, 2008) are given in Table 3. As NSM rectangular bars were cut out of the CFRP plates, their material properties are the same as those of the CFRP plates.

Test Setup

The test setup is shown in Fig. 4. The test wallettes were built separately and then placed on a steel I-beam for testing, with no mortar or other special connection provided between the wallette and the steel beam. The diagonal force was applied by means of a manually operated hydraulic actuator acting through a steel shoe placed at the top corner and was transferred to another loading shoe at the opposing bottom corner using two high-strength steel bars that were placed along each wallette face. Diagonal displacements were measured using two perpendicular portal gauges that were aligned along the wallette diagonals on the unretrofitted wall face. The wallettes were loaded continuously up to 50% of the expected maximum force, and in small increments (10–20% of the

peak force) afterwards until the maximum force was attained, which allowed cracks to be observed and photographs to be taken. In total, a test was completed within 90–120 minutes.

Experimental Results

General response of tested wallettes

Unretrofitted wallettes failed by the formation of diagonal cracks (Russell 2010). The failure was more sudden for wallette AP2, where following the formation of a crack, the wallette was not able to sustain any force. The force dropped gradually in wallettes AP4, AP6, AP7, and AP8 after the appearance of cracks, and the wall slid on the stepped cracks. The response of these wallettes can be considered a combined diagonal shear-sliding shear failure.

The shear stress (v) - %drift (δ) and horizontal force (F) - %drift (δ) responses of the retrofitted wallettes are shown and compared with the unretrofitted wallettes in Fig. 5. In each graph in Fig. 5, the response of the retrofitted wallette is indicated by the darker line and the responses of the unretrofitted wallettes are indicated by the lighter lines, with only one light line shown for stage 3 testing, as only one unretrofitted wallette (AP8) was tested in stage 3. The curves are plotted to a maximum drift of 3% only, as building codes typically limit the maximum lateral drift in buildings to approximately 3%. The shear stress, *v* was calculated as:

$$v = {(P\cos\alpha)}\Big/{\left(\frac{L+H}{2}\right)(t)} \qquad (1)$$

where P = applied diagonal force and α = angle between wallette top and applied force (45^o for stage 1 and stage 2, 42.6^o for stage 3).

It can be shown than the %drift, δ, which is the ratio of the horizontal displacement of the wallette top to the wallette height and is expressed as a percent, equals the shear strain, γ, which is calculated from the shortening, ΔS, measured along the applied force, the elongation, ΔL, measured perpendicular to the applied force, and the gauge length, g, as follows:

$$\delta = \gamma = {\Delta S + \Delta L}/{2g}\ (tan \propto + cot \propto) \quad (2)$$

Table 4 presents the values of horizontal reinforcement ratio, ρ_h, vertical reinforcement ratio, ρ_v, FRP modulus of elasticity, E_f, wallette maximum horizontal force, F_{max}, shear strength, v_{max}, increase in shear strength, Δv, percentage increase in shear strength, $\%\Delta v$, pseudo-ductility, μ, toughness, T, modulus of rigidity, G, Poisson's ratio, ν, and modulus of elasticity, E, for each wallette. Reinforcement ratios, ρ_h and ρ_v were computed as follows:

$$\rho_h = {(n)(t_f)(w_h)}/{(H)(t)} \ ; \ \rho_v = {(n)(t_f)(w_v)}/{(L)(t)} \quad (3)$$

where n = number of FRP layers; t_f = FRP thickness; $w_{h,v}$ = total length of FRP normal to horizontal (h) and vertical (v) axes respectively; H = wallette height; L = wallette length; and t = wallette thickness.

All wallettes exhibited an almost linear v-δ (or F-δ) response until about 50% of the maximum force, when, in many cases, narrow cracks appeared in the wallette. The stiffness then reduced steadily until the maximum force was reached, accompanied by the appearance of a major crack. The strength then dropped, and the wallettes deformed until the occurrence of significant out-of-plane displacements or large drifts, which led to termination of the test. A number of cracks had appeared in each wallette by the end of the test. Most wallettes failed by diagonal cracking, as is evident from the cracking pattern of the retrofitted wallettes (Fig. 6.), and a typical diagonal crack is shown in Fig. 7. The application of only horizontal CFRP did not inhibit the sliding shear mode.

The wallettes that were retrofitted on one surface only and failed by diagonal cracking exhibited an out-of-plane phase following the initial in-plane phase due to the eccentric stiffness resulting from the single-surface retrofit. The out-of-plane phase was often characterized by the part

of the wallette located above the main diagonal crack tilting towards the retrofitted face. This phenomenon is important for practical design of FRP retrofits of URM walls as the stability of the retrofitted wallettes was reduced and tests had to be stopped due to the potential danger of wallettes collapsing on the floor. Conversely, the out-of-plane displacement can be useful in providing advance failure warning to the residents of a building. No out-of-plane displacement was observed for the wallettes that had FRP applied on both surfaces and for the wallettes that deformed by sliding.

Debonding of FRP was observed in the wallettes that were retrofitted with CFRP plates. The presence of overlapped CFRP plates in some wallettes also resulted in lower bond strength at the interface of the two plates (Figure 8), and contributed to low shear strength resulting from premature debonding of CFRP.

Shear strength

Table 4 lists the shear strength, v_{max}, of both the unretrofitted and the FRP-retrofitted wallettes, tested in each stage. The increase in shear strength, Δv, is computed for each stage 1 and stage 2 retrofitted wallette as the difference between the shear strength of the retrofitted wallette and the average of the shear strength of the companion unretrofitted wallettes. Average values were not available for stage 3 testing because only one unretrofitted wallette (AP8) was tested, and hence the increase in shear strength is reported as the difference between the shear strength of a retrofitted wallette and the shear strength of the unretrofitted wallette (AP8). The maximum increase in shear strength (0.54 MPa) was achieved with full surface biaxial GFRP fabrics (WTG2). Also, a large increase in shear strength was attained with the other full surface GFRP fabrics (WTG1, WTG7, WTG8). Application of strips cut from the fabrics was less successful in increasing shear strength, except for the diagonal (WTG4) and grid (WTG6) configurations. Use of the NSM CFRP rectangular bars on both faces (WTC7) resulted in the highest strength increase (0.46 MPa) of all CFRP-retrofitted wallettes, with single-faced NSM CFRP being comparatively ineffective, thus indicating better performance when the NSM application was installed on both faces of the wallettes that failed by diagonal shear cracking. Significant shear strength increase was also obtained with the diagonal

configuration of CFRP plates (WTC4). A significant increase in shear strength was also obtained for wallettes with only vertical FRP elements due to a phenomenon known as dilation (Peterson et al. 2010), as FRP restrains masonry from dilating laterally. Overall, an increase in shear strength of 31–325% (0.11–0.54 MPa) of the unretrofitted wallette strength was achieved with the application of the various retrofit interventions.

The increase in shear strength, Δv, has a linear relationship with the product $(\rho_h)(E_f)$ (ICC Evaluation Service 2007). This relationship was explored in Figure 9 by plotting Δv for horizontally-retrofitted wallettes only against $(\rho_h)(E_f)$, and a good linear fit was obtained, which was in agreement with the previous research findings.

Pseudo-ductility

Ductility is the ability of a material to deform beyond the elastic range without fracturing or breaking and is an important parameter in seismic design. For materials without a distinct yield point, such as masonry, the concept of pseudo-ductility can be used. The yield drift, δ_{yield}, was determined from a bilinear equivalent elasto-plastic system (Fig. 10) with the same energy absorption as that of the wallette up to 80% of the strength in the post-peak region. The maximum available drift, δ_{avail}, is the post-peak drift at 80% of the strength. The available pseudo-ductility, μ, was hence calculated as the ratio of δ_{avail} to δ_{yield}. A similar concept has been used elsewhere (Marcari et al. 2007). The FRP retrofit interventions resulted in a large increase in pseudo-ductility (for values, see Table 4) for wallettes that failed by diagonal shear cracking, with large increases being achieved for two wallettes with only horizontal retrofits (WTG1 and WTC1), for the wallette with the grid of GFRP fabric strips (WTG6), and for the wallette with CFRP diagonal plates (WTC4). Relatively smaller pseudo-ductility values were achieved for the wallettes with NSM retrofits.

Toughness

Modulus of toughness, or simply, toughness, *T*, represents the energy per unit volume required to rupture a material and is a measure of the ductility and strength of a structure. Toughness is

computed here for each wallette as the area under the experimental v-δ curves (values of toughness given in Table 4). The FRP application substantially enhanced the toughness of the wallettes, and the increase was more significant for the wallettes that failed by diagonal shear cracking. Wallettes WTG2 and WTC7 that had the maximum increase in shear strength also showed high values of toughness, whereas lower values were obtained in general for the one-faced CFRP retrofits, except for the diagonal configuration (WTC4).

Stiffness

Modulus of rigidity, G, is a measure of stiffness of any material and is computed as the ratio of the shear stress to the corresponding shear strain. The modulus of rigidity was calculated here (values in Table 4) as the secant modulus of the v-δ curve up to 70% of strength. The stiffness of retrofitted wallettes was generally found to match the unretrofitted equivalent, with variations attributed to the natural variability of masonry rather than being due to the characterization of the retrofit scenario. Low values of stiffness were obtained for the NSM CFRP-retrofitted wallettes, because these wallettes had a low reinforcement ratio and hence the NSM FRP did not significantly increase the wallette stiffness.

Poisson's ratio, ν, is the ratio of the strain perpendicular to the applied force to the strain parallel to the applied force. Poisson's ratio is a useful parameter for design and analytical modeling of structures and can also be used to indirectly calculate the modulus of elasticity, E. The Poisson's ratio values were calculated (see Table 4) for the retrofitted wallettes only as the ratio of ΔL to ΔS at 40% of the maximum force, in accordance with the ASTM procedure for the calculation of Poisson's ratio of concrete in compression (ASTM 2002). No data was available for the unretrofitted wallettes. Low values were obtained for stage 1 wallettes, however the values were significantly higher for stage 2 and stage 3 wallettes. The E values were computed as follows, and the values are shown in Table 4:

$$E = 2\,(1 + \upsilon)\,G \tag{4}$$

Modulus of elasticity of masonry is reported in the literature as a function of the masonry compression strength, f'_m, and was determined to equal 268 f'_m for the type of masonry used in this research, by conducting axial compression tests on masonry prisms and recording stress and strain data. By using the mean value of f'_m measured for this experimental study (7.1 MPa), an average E value of 1.89 GPa was obtained, which is higher than the average E value of retrofitted wallettes (1.39 GPa), confirming little benefit from FRP in enhancing the stiffness of URM.

Discussion

Exact comparison of the results of this research with previously reported testing is difficult due to the different masonry materials, wallette sizes and test configuration used here. Previous tests have indicated no or limited strength gain with FRP, inefficiency of single-faced retrofit, or increase in strength with both single-faced and double-faced retrofits. This research showed that both single-faced and double-faced FRP was effective in increasing shear strength of URM wallettes by up to 325%, which was greater than the increase achieved in previous research. Li et al. (2005) and Turco et al. (2006) reported an increase with NSM GFRP pultruded circular bars in the wall pseudo-ductility, which was computed as the ratio of the ultimate displacement to the yield displacement. A different method was used in this research to compute pseudo-ductility employing 'maximum available drift' rather than 'maximum displacement', which may not be available due to severe damage to the wall. High values of pseudo-ductility were obtained in this research. No data for toughness has been reported elsewhere. Santa Maria et al. (2004) reported a large scatter in modulus of rigidity values, but indicated a mean increase in modulus of rigidity values with diagonal FRP elements. Mixed results were obtained here for modulus of rigidity.

The cost of GFRP fabrics is significantly lower than CFRP pultruded elements, and also fabrics are simpler to install due to ease in handling and cutting, reduced surface preparation and less training required for installation. This research has shown that for the same increase in shear strength (Table 4 and Figure 9), less pultruded CFRP area is required due to CFRP's higher stiffness,

potentially making CFRP pultruded systems more suitable for seismic retrofit of historical structures. NSM pultruded bars offer a solution to minimize visual impact on a structure, as these bars can be 'hidden' within the bed joints for horizontal retrofits. The amount of NSM retrofit may however be limited by the mortar joint size, and also the installation of NSM retrofit is labor-intensive. Full surface fabrics were beneficial in holding the wall together over a large range of drift, minimizing wall damage and significantly increasing the shear strength and toughness. Only common commercially used FRP systems were investigated in order to make this research useful for designers, and hence fiber anchors were used only with GFRP fabrics.

The FRP systems were successful in enhancing the parameters that are important in a seismic retrofit program, other than stiffness. Guidance for seismic retrofit design can be obtained from the results. For example, a combination of horizontal and vertical fabrics with full surface coverage provides the greatest increase in shear strength and a moderate increase in pseudo-ductility. If only increase in pseudo-ductility is the main goal, use of only horizontal full surface fabrics or diagonal CFRP plates is recommended, and such systems also result in significant shear strength increase. Future work involving reverse cyclic testing would also be beneficial for confirmation of these findings.

Conclusions

- FRP systems are viable options for seismic retrofit interventions of URM, as was observed by the enhancement of parameters important for improving seismic behavior of URM.
- A large increase in shear strength, up to 325%, was achieved with FRP. The use of FRP on only one face was effective, however significantly large out-of-plane displacements were observed in wallettes that failed by diagonal shear cracking. This aspect has also been observed by other researchers.
- The FRP application greatly enhanced the pseudo-ductility and toughness, especially of those wallettes that failed by diagonal shear cracking.

- Horizontal FRP, if used on walls with a weak mortar, does not mitigate the sliding deformation mode of URM. The use of vertical or diagonal FRP retrofit with or without horizontal FRP restrains the wallettes from sliding, as was previously observed by other researchers. Vertical FRP was also effective in increasing the shear strength.
- Insignificant change in stiffness was observed with FRP.
- FRP debonding was more significant in wallettes with CFRP plates.
- A linear relationship exists between the increase in shear strength and the product of horizontal reinforcement ratio and FRP modulus of elasticity. This aspect was studied in this research only for horizontally-retrofitted wallettes, and the results confirmed the previously reported work.

Acknowledgements

The authors wish to acknowledge the financial support of the New Zealand Foundation for Research, Science and Technology (FRST), the Building Research Association of New Zealand (BRANZ), and the Higher Education Commission of Pakistan (HEC). The authors also wish to thank Fyfe Co. LLC and Sika AG for donating FRP, Golden Bay Cement for their donation of cement, and Alistair Russell and Ronald Lumantarna for their help during the experimental program and allowing the authors to include their test results. Support provided by Building Chemical Supplies and Contech New Zealand pertaining to supply and installation of FRP is also gratefully acknowledged.

References

Alcaino, P., and Santa-Maria, H. (2008). "Experimental response of externally retrofitted masonry walls subjected to shear loading." *Journal of Composites for Construction*, 12(5), 489-498.

ASTM (2002). "ASTM C109/C109M-02 Standard test method for compressive strength of hydraulic cement mortars (using 2-in. or [50-mm] cube specimens)." *ASTM International*, West Conshohocken, Pa.

ASTM (2002). "ASTM C469-02 Standard test method for static modulus of elasticity and Poisson's ratio of concrete in compression." *ASTM International*, West Conshohocken, Pa.

ASTM (2002). "ASTM E519-02 Standard test method for diagonal tension (shear) in masonry assemblages." *ASTM International*, West Conshohocken, Pa.

ASTM (2003). "ASTM C270-03 Standard specification for mortar for unit masonry." *ASTM International*, West Conshohocken, Pa.

ASTM (2003). "ASTM C1314-03a Standard test method for compressive strength of masonry prisms." *ASTM International*, West Conshohocken, Pa.

Bruneau, M. (1994). "State-of-the-art report on seismic performance of unreinforced masonry buildings." *Journal of Structural Engineering*, 120(1), 230-251.

Dowrick, D. J. (1998). "Damage and intensities in the magnitude 7.8 1931 Hawke's Bay, New Zealand, earthquake." *Bulletin of the New Zealand National Society for Earthquake Engineering*, 31(3), 139-162.

Drysdale, R. G., Hamid, A. H., and Baker, L. R. (1999). "Masonry structures: behaviour and design." *The Masonry Society*, Boulder, Colo.

Elgawady, M. A., Lestuzzi, P., and Badoux, M. (2005). "In-plane seismic response of URM walls upgraded with FRP." *Journal of Composites for Construction*, 9(6), 524-535.

Fyfe Co. LLC (2009). "Tyfo SEH Fibr Anchors using Tyfo S Epoxy." *Fyfe Co. LLC*, San Diego, Calif.

Fyfe Co. LLC (2009). "Tyfo WEB Composite using Tyfo S Epoxy." *Fyfe Co. LLC*, San Diego, Calif.

Fyfe Co. LLC (2010). "Tyfo SEH-51A Composite using Tyfo S Epoxy." *Fyfe Co. LLC*, San Diego, Calif.

Hamid, A. A., El-Dakhakhni, W. W., Hakam, Z. H. R., and Elgaaly, M. (2005). "Behavior of composite unreinforced masonry-fiber-reinforced polymer wall assemblages under in-plane loading." *Journal of Composites for Construction*, 9(1), 73-83.

Hamilton, H. R., and Dolan, C. W. (2001). "Flexural capacity of glass FRP strengthened concrete masonry walls." *Journal of Composites for Construction*, 5(3), 170-178.

Haroun, M. A., and Mosallam, A. S. (2002). "Cyclic shear test of multi-wythe existing brick wall: retrofitted by a single layer of TYFO SEH-51A applied on one side." Report no. FYFE-MW, *Fyfe Co. LLC*, San Diego, Calif.

Hendry, A. W., Sinha, B. P., and Davies, S. R. (1997). "Design of masonry structures." *E & FN SPON (An Imprint of Chapman & Hall)*, London, U.K.

Holmes, I. L. (1965). "Concrete masonry buildings in New Zealand." *Proc., Third World Conference on Earthquake Engineering (3WCEE)*, New Zealand National Committee on Earthquake Engineering, Wellington, New Zealand, IV-244–IV-255.

ICC Evaluation Service (2007). "Acceptance criteria for concrete and reinforced and unreinforced masonry strengthening using fiber reinforced polymer (FRP) composite systems (AC125)." *ICC Evaluation Service*, Whittier, Calif.

Javed, M., Khan, A. N., Penna, A., and Magenes, G. (2006). "Behaviour of masonry structures during the Kashmir 2005 Earthquake." *Proc., First European Conference on Earthquake Engineering and Seismology (1st ECEES)*, European Association of Earthquake Engineering and European Seismological Commission, Geneva, Switzerland, Paper no. 1077.

Kuzik, M. D., Elwi, A. E., and Cheng, J. J. R. (2003). "Cyclic flexure tests of masonry walls reinforced with glass fiber reinforced polymer sheets." *Journal of Composites for Construction*, 7(1), 20-30.

Li, T., Galati, N., Tumialan, J. G., and Nanni, A. (2005). "Analysis of unreinforced masonry concrete walls strengthened with glass fiber-reinforced polymer bars." *ACI Structural Journal*, 102(4), 569-577.

Magenes, G., and Calvi, G. M. (1997). "In-plane seismic response of brick masonry walls." *Earthquake Engineering and Structural Dynamics*, 26(11), 1091-1112.

Marcari, G., Manfredi, G., Prota, A., and Pecce, M. (2007). "In-plane shear performance of masonry panels strengthened with FRP." *Composites Part B: Engineering*, 38(7-8), 887-901.

Marshall, O. S., Jr., Sweeney, S. C., and Trovillion, J. C. (2000). "Performance testing of fiber-reinforced polymer composite overlays for seismic rehabilitation of unreinforced masonry walls (ERDC/CERL TR-00-18)." *Construction Engineering Research Laboratory (CERL), Engineer Research and Development Center, US Army Corps of Engineers*, Champaign, Ill.

Peterson, R. B., Masia, M. J., and Seracino, R. (2010). "In-plane shear behavior of masonry panels strengthened with NSM CFRP strips: experimental investigation." *Journal of Composites for Construction*, 10.1061/(ASCE)CC.1943-5614.0000134 (April 28, 2010).

Rossetto, T., and Peiris, N. (2009). "Observations of damage due to the Kashmir Earthquake of October 8, 2005 and study of current seismic provisions for buildings in Pakistan." *Bulletin of Earthquake Engineering*, 7(3), 681-699.

Russell, A. P. (2010). "Characterisation and seismic assessment of unreinforced masonry buildings." PhD thesis, University of Auckland, Auckland, New Zealand.

Russell, A. P., and Ingham, J. M. (2010). "Prevalence of New Zealand's unreinforced masonry buildings." *Bulletin of the New Zealand Society for Earthquake Engineering*, 43(3), 192-207.

Santa-Maria, H., Duarte, G., and Garib, A. (2004). "Experimental investigation of masonry panels externally strengthened with CFRP laminates and fabric subjected to in-plane shear load." *Proc., Thirteenth World Conference on Earthquake Engineering (13WCEE)*, Canadian Association for Earthquake Engineering and International Association for Earthquake Engineering (IAEE), Vancouver, Canada, Paper no. 1627.

Schwegler, G. (1995). "Masonry construction strengthened with fiber composites in seismically endangered zones." *Proc., 10th European Conference on Earthquake Engineering (10ECEE)*, Balkema, Vienna, Austria, 2299-2303.

Seki, M., Vacareanu, R., Saito, T., Cotofana, D., Lozinca, E., Popa, V., and Chesca, A. B. (2008). "Cyclic shear tests on plain and FRP retrofitted masonry walls." *Proc., 14th World Conference on Earthquake Engineering (14WCEE)*, International Association for Earthquake Engineering, Beijing, China.

Sika Corporation (2005). "Sika Carbodur: Carbon fiber laminate for structural strengthening (Identification no. 332)." *Sika Corporation*, Lyndhurst, N.J.

Sika Corporation (2008). "Sikadur 30: High-modulus, high-strength, structural epoxy paste adhesive for use with Sika CarboDur reinforcement. (Identification no. 332-15)." *Sika Corporation*, Lyndhurst, N.J.

Silva, P. F., Yu, P., and Nanni, A. (2008). "Monte Carlo simulation of shear capacity of URM walls retrofitted by polyurea reinforced GFRP grids." *Journal of Composites for Construction*, 12(4), 405-415.

Stratford, T., Pascale, G., Manfroni, O., and Bonfiglioli, B. (2004). "Shear strengthening masonry panels with sheet glass-fiber reinforced polymer." *Journal of Composites for Construction*, 8(5), 434-443.

To-Nan, C., Ja-Shian, C., Yen-Chih, L., and Yu-Chun, L. (2006). "Performance of URM walls strengthened with CFRP under horizontal cyclic loading." *Proc., First European Conference on*

Earthquake Engineering and Seismology (1st ECEES), European Association of Earthquake Engineering and European Seismological Commission, Geneva, Switzerland, Paper no. 299.

Turco, V., Secondin, S., Morbin, A., Valluzzi, M. R., and Modena, C. (2006). "Flexural and shear strengthening of un-reinforced masonry with FRP bars." *Composites Science and Technology*, 66(2), 289-296.

Valluzzi, M. R., Tinazzi, D., and Modena, C. (2002). "Shear behavior of masonry panels strengthened by FRP laminates." *Construction and Building Materials*, 16(7), 409-416.

Table 1: Literature review of diagonal compression tests of FRP-retrofitted URM wallettes.

Reference	Wallette properties				γ	FRP system				% increase in strength	Failure mode
	Material	L (mm)	H (mm)	N		Mat-erial	Application method and FRP form	θ	RF		
Marshall et al. (2000)	Block/ hollow brick	1220 1220	1220 1220	1 2	45	G/C/ GVA	EB fabric/ grid	0/ 90	1	(-30)–34	DS/LC
Valluzzi et al. (2002)	Solid brick	515	510	1	45	G/C/ PVA	EB fabric	45/ 0+90	1/2	(-10)–74	DS
Santa Maria et al. (2004)	Hollow brick	1060	1100	1	0	C	EB plate/ fabric	0/ 45	1/2	0–70	DS/LC /S
Hamid et al.(2005)	Block	Size not mentioned		1	45	G	EB fabric	0+90	2	≤358	LC
Li et al. (2005)	Block	1625	1625	1	0	G	NSM bar/plate	0 /0 +90	1/2	28–123	DS/S
Turco et al.(2006)	Block	1600	1600	1	0	G	NSM bar	0	1/2	70–123	DS/S
Silva et al. (2008)	Block/ grouted brick	1626	1219	1	0	G	EB polyurea bonded grid	0/90	1/2	21–99	DS/S
Peterson et al. (2010)	Solid brick	1200	1200	1	45	C	NSM rectangular strip	0/90/ 0+90	1/2	(-18)–36	DS/S

Note: Block = concrete block; brick = burnt-clay brick; L = wallette length; H = wallette height; N = number of wythes; γ = Angle in degrees during test between wall bed joints and floor; G = glass; C = carbon; GVA = glass vinyl ester; PVA = polyvinyl alcohol; EB = externally-bonded; NSM = near-surface mounted; θ = angle in degrees between FRP fiber and wall bed joints; RF = number of retrofitted wallette faces; DS = diagonal shear; S = sliding; LC = local cracking.

Table 2: Wallette dimensions and FRP retrofit details.

Stage	Wallette	Wallette dimensions (mm)			Retrofit details (FRP applied on one face only except for WTC7 and WTC9)	
		L	H	t	Retrofitted with (number of FRP layers shown within parentheses)	Pattern
1	AP2	1170	1170	225	-	-
	AP4				-	-
	WTG1				Full surface GFRP fabric (2)	HL
	WTG2				Full surface GFRP fabric (2)	HL+V
	WTG3				Four 105 mm wide strips cut out of GFRP fabrics (2)	HL
	WTG4				Two 150 mm wide strips cut out of GFRP fabrics (2)	D
	WTG5				Four 105 mm wide strips cut out of GFRP fabrics (2)	V
2	AP6	1170	1170	225	-	-
	AP7				-	-
	WTC1				Five 50 mm wide CFRP plates (1)	HL
	WTC2				Six 50 mm wide (pairs of two) CFRP plates (1)	HL
	WTC3				Six 50 mm wide CFRP plates (1)	G
	WTC4				Two 125 mm wide CFRP plates (1)	D
	WTC5				Six 50 mm wide (pairs of two) CFRP plates (1)	V
	WTG6				Six 75 mm wide strips cut out of GFRP fabrics (2)	G
	WTG7				Two full surface GFRP fabrics (2)	V
3	AP8	1170	1075	225	-	-
	WTC6				Five 1.2 mm x 15 mm NSM bars (1)	V
	WTC7				Five 1.2 mm x 15 mm NSM bars *on both faces*(1)	V
	WTC8				Five 1.2 mm x 15 mm NSM bars (1)	HL
	WTC9				Five 1.2 mm x 15 mm NSM bars *on both faces* (1)	HL
	WTG8				Full surface GFRP fabrics (2)	B

Note: t = wallette thickness; HL = horizontal; V = vertical; D = diagonal; G = grid; and B = biaxial.

Table 3: Material properties.

Average compressive strength and standard deviation (SD) of masonry materials						
Stage	**Mortar (MPa)**		**Brick (MPa)**		**Masonry (MPa)**	
	Strength	**SD**	**Strength**	**SD**	**Strength**	**SD**
1	3.2	1.3	13.5	6.0	8.3	3.4
2	1.8	0.7	11.2	4.8	5.4	1.2
3	1.4	0.4	21.2	8.8	8.8	2.8
FRP (manufacturer-provided typical test values)						
Property	**Uniaxial GFRP fabric**		**Biaxial GFRP fabric**		**CFRP plates and rectangular bars**	
Dry fiber						
Tensile strength, MPa	3240		3240		-	
Tensile modulus, GPa	72.4		72.4		-	
Ultimate elongation, %	4.5		4.5		-	
Weight, g/m^2	915		295		-	
Epoxy						
Tensile strength, MPa	72.4		72.4		24.8 (at seven days)	
Tensile modulus, GPa	3.2		3.2		4.5 (at seven days)	
Ultimate elongation, %	5.0		5.0		1.0 (at seven days)	
Composite						
Tensile strength in primary fiber direction, MPa	575		309		3100	
Tensile strength normal to primary fiber direction, MPa	25.8		309			
Tensile modulus, GPa	26.1		19.3		165	
Elongation at break, %	2.2		1.6		1.69	
Laminate thickness, mm	1.3		0.25		1.2	

Table 4: Experimental results.

Stage	Wallette	ρ_h	ρ_v	E_f	F_{max}	v_{max}	Δv	$\%\Delta v$	μ	T	G	ν	E
		X10^{-3}	*X10^{-3}*	*GPa*	*kN*	*MPa*	*MPa*			*J/m^3*	*GPa*		*GPa*
1	AP2	-	-	-	149	0.56	-	-	1.0	0.18	0.71	NA	NA
	AP4	-	-	-	107	0.39	-	-	1.0	0.77	0.35	NA	NA
	WTG1	11.6	0	26.1	205	0.78	0.30	63	17.5	13.46	0.98	0.01	1.98
	WTG2	5.8	5.8	26.1	269	1.02	0.54	114	5.6	24.68	0.65	0.01	1.31
	WTG3	0	4.1	26.1	165	0.63	0.15	31	6.8	20.53	0.52	0.01	1.05
	WTG4	2.1	2.1	26.1	198	0.75	0.28	58	6.0	14.09	0.65	0.03	1.34
	WTG5	4.1	0	26.1	172	0.65	0.17	36	6.5	18.48	0.43	0.01	0.87
2	AP6	-	-		36	0.13	-	-	12.8	1.64	0.89	NA	NA
	AP7	-	-	-	35	0.13	-	-	8.6	1.10	1.57	NA	NA
	WTC1	1.1	0	165.0	76	0.29	0.16	119	13.8	6.29	0.95	0.08	2.05
	WTC2	1.4	0	165.0	92	0.35	0.22	166	6.5	3.74	0.92	0.13	2.08
	WTC3	0.7	0.7	165.0	98	0.37	0.24	183	10.3	9.34	0.97	0.11	2.15
	WTC4	0.8	0.8	165.0	119	0.45	0.32	245	15.6	15.90	1.22	0.40	3.42
	WTC5	0	1.4	165.0	111	0.42	0.29	221	10.9	9.40	0.72	0.24	1.79
	WTG6	2.2	2.2	26.1	105	0.40	0.27	202	18.0	12.19	0.85	0.10	1.87
	WTG7	0	11.6	26.1	124	0.47	0.34	259	5.0	17.84	0.35	0.19	0.83
3	AP8	-	-	-	37	0.14	-	-	17.1	1.13	0.69	NA	NA
	WTC6	0	0.3	165.0	79	0.31	0.17	121	6.6	13.04	0.20	0.13	0.45
	WTC7	0	0.7	165.0	153	0.61	0.46	325	3.4	19.41	0.08	0.35	0.22
	WTC8	0.4	0	165.0	65	0.26	0.11	80	9.3	9.40	0.22	0.26	0.55
	WTC9	0.7	0	165.0	67	0.27	0.12	86	4.6	7.74	0.25	0.52	0.76
	WTG8	2.2	2.2	19.3	81	0.32	0.18	125	11.2	13.90	0.26	0.79	0.93

Note: ρ_h = horizontal reinforcement ratio; ρ_v = vertical reinforcement ratio; E_f = FRP elastic modulus; F_{max} = Horizontal component of maximum applied force; v_{max} = shear stress; Δv = increase in shear strength due to FRP application; $\%\Delta v$ = percent increase in shear strength with respect to the average shear strength of companion unreinforced wallettes; μ = pseudo-ductility; T = modulus of toughness; G = modulus of rigidity; ν = Poisson's ratio; NA = data not available; and E = modulus of elasticity.

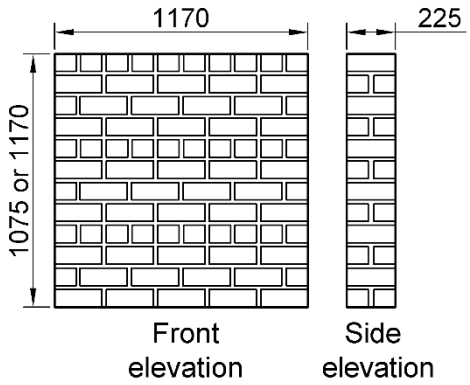

Figure 1: Wallette dimensions (mm) and masonry bond pattern.

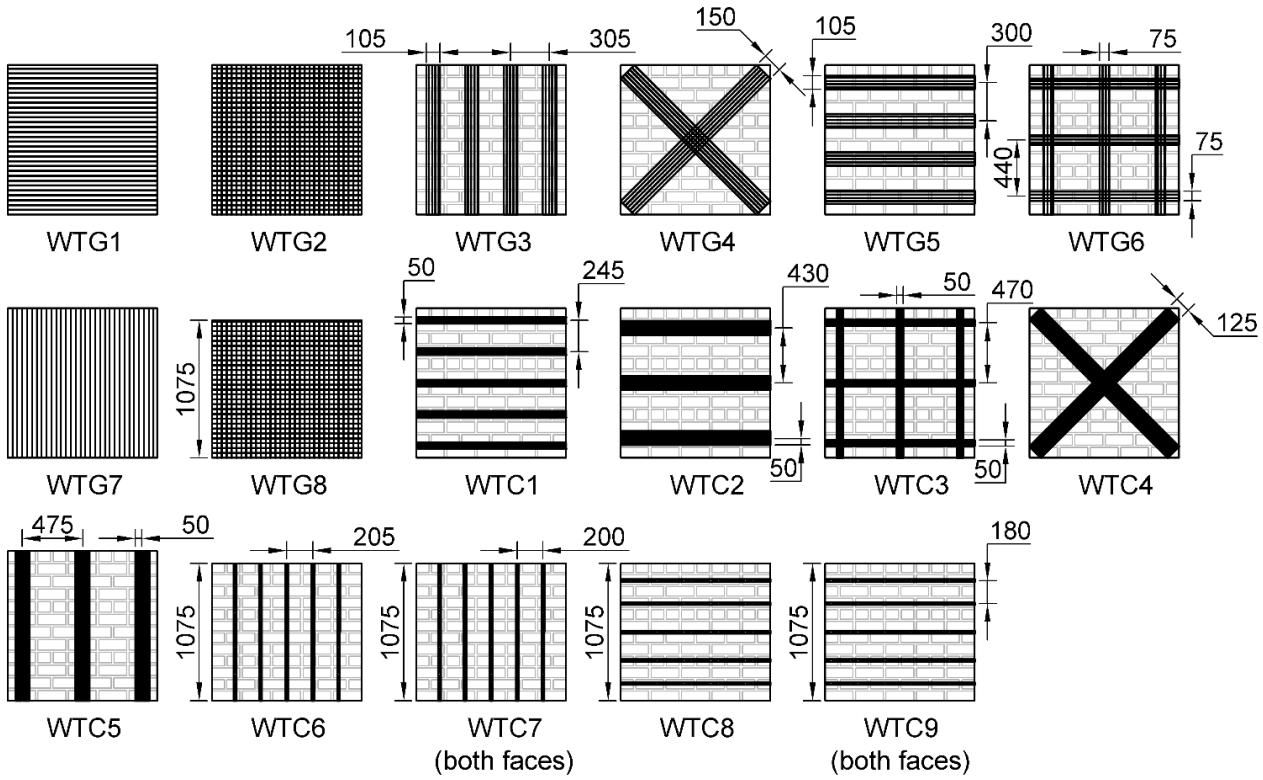

Figure 2: FRP retrofit details (all dimensions in mm). Wallette height is 1170 mm unless otherwise noted.

Figure 3: Installation of glass fabric on a wall that was retrofitted similarly to the test wallettes.

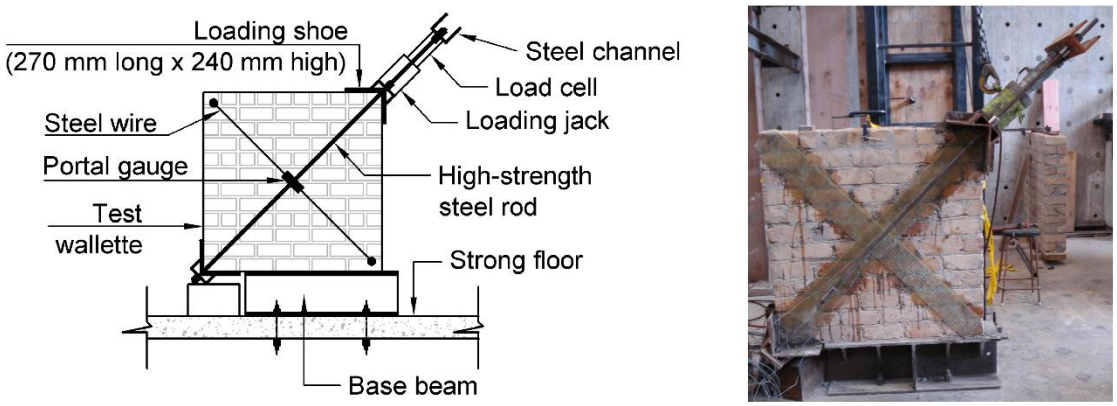

Figure 4: Test setup. For clarity, only one of the two portal gauges is shown. The other portal gauge was located behind the high-strength steel rod.

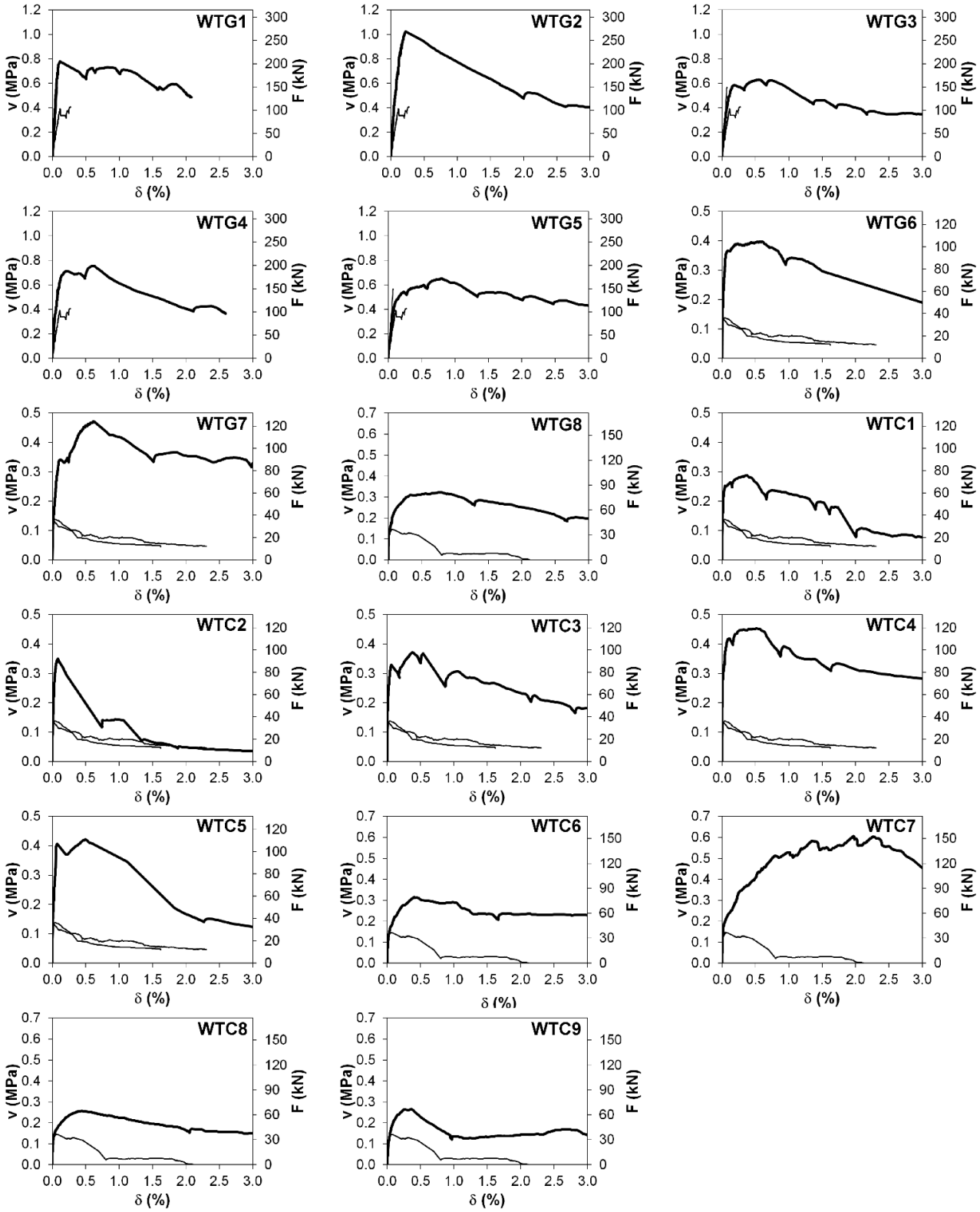

Figure 5: Shear stress (v) - %drift (δ) plots for FRP-retrofitted wallets. Curves for companion wallettes are shown in lighter shades.

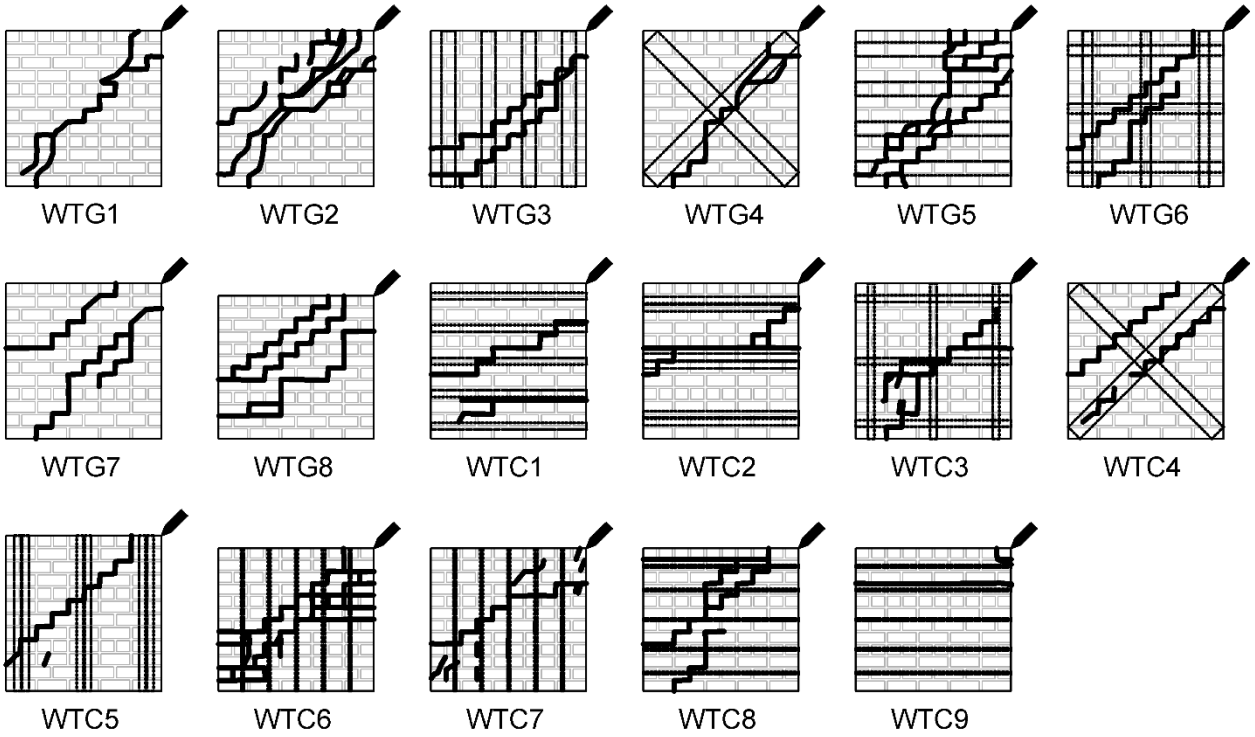

Figure 6: Cracking patterns of FRP-retrofitted walls.

Figure 7: Diagonal crack in a wallette.

Figure 8: Debonding of CFRP plate.

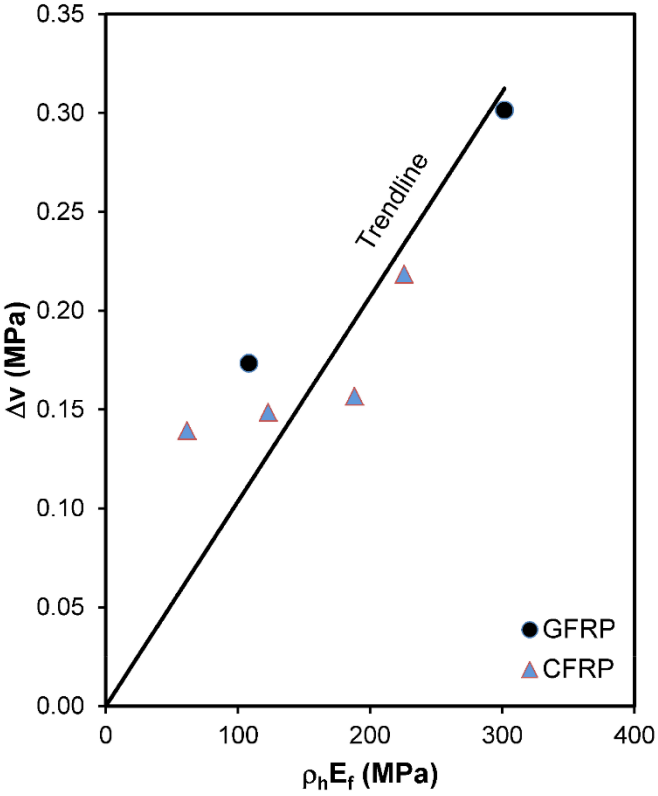

Figure 9: Increase in shear strength versus product of horizontal reinforcement ratio and FRP modulus of elasticity plot for horizontally-reinforced wallettes.

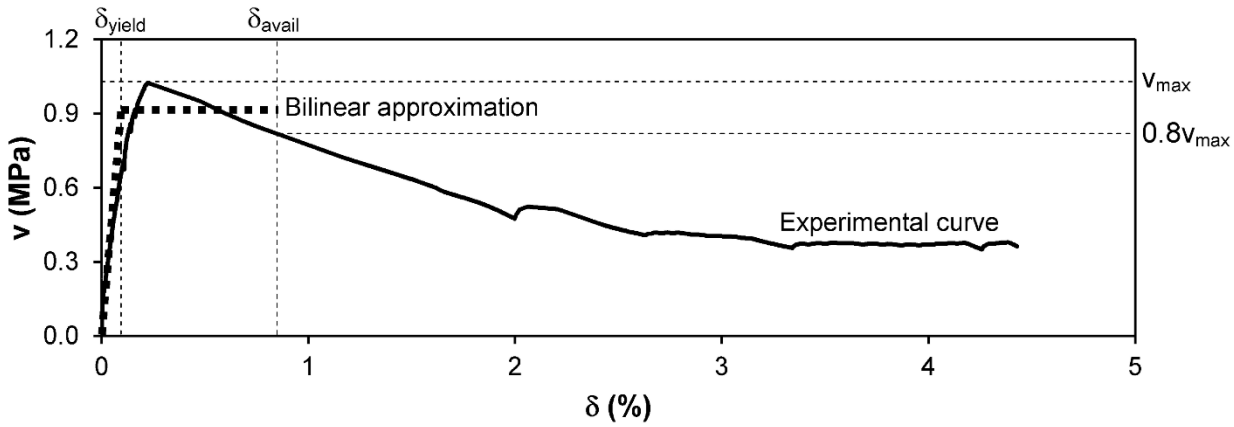

Figure 10: Bilinear approximation of experimental curve for wallette WTG2.